DALTON

1,2-Di-*tert*-butyltetrafluorodisilane, $Bu^tSiF_2SiF_2Bu^t$: vibrational spectra and molecular structure in the gas phase by electron diffraction and *ab initio* calculations†

Bruce A. Smart,[a] Heather E. Robertson,[a] Norbert W. Mitzel,[a] David W. H. Rankin,*[,a] Robert Zink[b] and Karl Hassler*[,b]

[a] *Department of Chemistry, University of Edinburgh, West Mains Rd., Edinburgh, UK EH9 3JJ*
[b] *Institut für Anorganische Chemie, Technische Universität Graz, Stremayrgasse 16, A-8010 Graz, Austria*

The molecular structure of 1,2-di-*tert*-butyltetrafluorodisilane, $Bu^tSiF_2SiF_2Bu^t$, has been determined in the gas phase by electron diffraction (GED) and *ab initio* molecular orbital calculations. Together with infrared and Raman studies, GED shows that only a single conformer (*anti*, C_{2h} symmetry) is present in the gas phase. From normal coordinate analysis, the Si–Si stretching force constant is 179 N m^{-1}, within the range previously observed for other related compounds. Important structural parameters (r_a) are: Si–Si 234.6(6), Si–C 187.2(3), Si–F 160.0(2), C–C 153.7(3), C–H 113.5(2) pm, Si–Si–C 114.6(7), Si–Si–F 108.7(3) and F–Si–F 107(2)°. This geometry is supported by theoretical predictions obtained at the 6-31G*/SCF level.

In recent years, rotational isomerism about silicon–silicon bonds has been the focus of a great deal of attention. Conformational effects on the electronic spectra of peralkylated silicon backbone polymers in the near-UV region are surprisingly large[1] and considerable variations of the absorption bands have been observed as a function of Si-backbone conformations for both polysilanes and short-chain silanes such as decamethyl-*n*-tetrasilane.[2] Previous calculations (6-31G*/MP2) on decamethyl-*n*-tetrasilane predict the presence of three pairs of enantiomeric conformers with the silicon backbone forming dihedral angles of around ±60° (*gauche*, $E_{rel.} = 0.4$ kJ mol^{-1}), ±90° (termed *ortho* by the authors, $E_{rel.} = 2.7$ kJ mol^{-1}) and ±165° (*anti*, $E_{rel.} = 0$ kJ mol^{-1}), although no indication of the presence of the *ortho* conformer could be deduced from IR matrix-isolation spectra.[2] Similarly, only two conformers (separated by 2.26 ± 0.15 kJ mol^{-1}) were observed in a variable-temperature Raman spectroscopic study of decamethyl-*n*-tetrasilane.[3] The absence of a third conformer in the vibrational spectra is probably due to the barrier separating *gauche* and *ortho* conformers lying below the ground state vibrational level.[2,4]

The existence of a potential energy minimum corresponding to an *ortho* conformer for Si_4Me_{10} (and also for C_4F_{10}, see ref. 5) has been rationalised in terms of 1,4 interactions of the substituents.[2] If 1,4 substituent interactions are responsible for the existence of three pairs of enantiomeric conformers on the potential energy surface of Si_4Me_{10}, an analogous potential energy distribution might apply to $Me_3C–SiMe_2–SiMe_2–CMe_3$ as well as other $Me_3C–SiX_2–SiX_2–CMe_3$ compounds (where X = H, F, Cl, Br or I).

Currently we are undertaking a series of vibrational and structural studies of novel disilanes directed at understanding the conformational behaviour of these interesting compounds. In this paper we report the results of a combined electron diffraction, *ab initio* and vibrational spectroscopic study of 1,2-di-*tert*-butyltetrafluorodisilane.

† Dedicated to Professor Dr. H. Bürger on the occasion of his 60th birthday.

Experimental

Synthesis

A sample of $Bu^tSiF_2SiF_2Bu^t$ was prepared according to the literature method.[6]

Ab initio calculations

All calculations were performed on a Dec Alpha 1000 4/200 workstation using the GAUSSIAN 94 program.[7] An extensive search of the torsional potential of 1,2-di-*tert*-butyltetrafluorodisilane was undertaken at the 3-21G*/SCF level in order to locate all structurally stable conformations. Two non-equivalent conformers, *anti* (C_{2h} symmetry) and *gauche* (C_2 symmetry), were located. These two conformers along with the transition state connecting these structures (also C_2 symmetry) were considered for further studies.

Geometry optimisations were undertaken at the SCF level using the standard 3-21G*[8–10] and 6-31G*[11–13] basis sets. Owing to the size of this molecule, calculations at the MP2 level were restricted to determination of single-point energies of the optimised 6-31G*/SCF geometries. Vibrational frequencies were calculated from analytic second derivatives at the 3-21G*/SCF and 6-31G*/SCF levels to determine the nature of stationary points, to provide estimates of amplitudes of vibration (u) for use in the GED refinements and for comparison with experimentally determined frequencies.

Infrared and Raman spectra

Infrared spectra in the range 3000–250 cm^{-1} were measured with a Perkin-Elmer 883 spectrometer using a film of pure liquid between CsBr plates. The Raman spectra were recorded with a Jobin Yvon T64000 triple monochromator (0.64 m focal length, used in the subtractive mode) employing a charge coupled device (CCD) camera. The sample was distilled into a 1 mm diameter capillary glass tube and sealed under a nitrogen atmosphere. The spectra were recorded using the 514.5 nm line of an argon-ion laser employing a 90° geometry. Variable-temperature spectra were obtained by mounting the capillary

on a copper block equipped with a heater and a thermocouple. Liquid nitrogen was used for cooling the sample.

Electron diffraction measurements

Electron scattering intensities were recorded on Kodak Electron Image plates using the Edinburgh gas-diffraction apparatus operating at *ca.* 44.5 kV (electron wavelength *ca.* 5.6 pm).[14] Nozzle-to-plate distances for the metal inlet nozzle were *ca.* 95 and 259 mm yielding data in the *s* range 20–356 nm^{-1}; three plates were exposed at each camera distance. The sample and nozzle temperatures were maintained at 293 K during the exposure periods.

The scattering patterns of benzene were also recorded for the purpose of calibration; these were analysed in exactly the same way as for $Bu^tSiF_2SiF_2Bu^t$ so as to minimise systematic errors in the wavelengths and camera distances. Nozzle-to-plate distances, weighting functions used to set up the off-diagonal weight matrix, correlation parameters, final scale factors and electron wavelengths for the measurements are collected in Table 1.

The electron-scattering patterns were converted into digital form using a computer-controlled Joyce Loebl MDM6 microdensitometer with a scanning program described elsewhere.[15] The programs used for data reduction[15] and least-squares refinement[16] have been described previously; the complex scattering factors were those listed by Ross *et al.*[17]

Results

Theoretical computations

A series of *ab initio* molecular orbital calculations was undertaken to investigate the structure of 1,2-di-*tert*-butyltetrafluorodisilane (shown in Fig. 1). An extensive search of the torsional potential led to the location of two conformers [*anti*, τ(C–Si–Si–C) 180, and *gauche*, τ(C–Si–Si–C) 138°]. Vibrational frequency calculations at the 6-31G*/SCF level indicate that both forms represent local minima. The molecular geometries of both conformers and the transition state to their interconversion are presented in Table 2. Owing to the size of this molecule, geometry optimisations could be undertaken at the SCF level only. Nevertheless, since this system has no significant multiple bond character and since lone pairs of electrons are present only on terminal atoms, it is expected that satisfactory estimates of molecular parameters should be obtained at this level.[18]

At the highest level of calculation employed (6-31G*/SCF), the *anti* and *gauche* conformers are predicted to have C–Si–Si–C dihedral angles of 180.0° and 138.3°, respectively. For the *gauche* isomer, this dihedral angle is far from the standard value of 60° at both levels employed; it is 123.3° at the 3-21G*/SCF level, and only deviates from an eclipsed arrangement by about 2° at the 3-21G*/SCF level or by slightly more than 15° at the 6-31G*/SCF level. The relatively small difference between the values of the dihedral angles for *anti* and *gauche* arrangements results in values of other geometric parameters varying by less than 0.5 pm or 0.5° between the two structures at the 6-31G*/SCF level.

The possibility that the potential energy barrier between the *anti* and *gauche* forms might be very small prompted us to search for the transition state connecting *anti* and *gauche* conformers. Vibrational frequency calculations were undertaken to verify that the located stationary point represented a true transition state on the PES (1 imaginary frequency) at both the 3-21G*/SCF (20*i* cm^{-1}) and 6-31G*/SCF levels (10*i* cm^{-1}). Values for all molecular parameters of the transition state (except for C–Si–Si–C) were predicted to be close to those found for the two local minima (see Table 2). The C–Si–Si–C dihedral angle

Table 1 Nozzle-to-plate distances (mm), weighting functions (nm^{-1}), correlation parameters, scale factors and electron wavelengths (pm) used in the electron diffraction study

Nozzle-to-plate distance	94.86	259.48
Δs	4	2
s_{min}	80	20
sw_1	100	40
sw_2	304	140
s_{max}	356	164
Correlation parameter	0.330	0.009
Scale factor[b]	0.631(13)	0.823(9)
Electron wavelength	5.639	5.640

[a] Determined by reference to the scattering pattern of benzene vapour. [b] Values in parentheses are the estimated standard deviations.

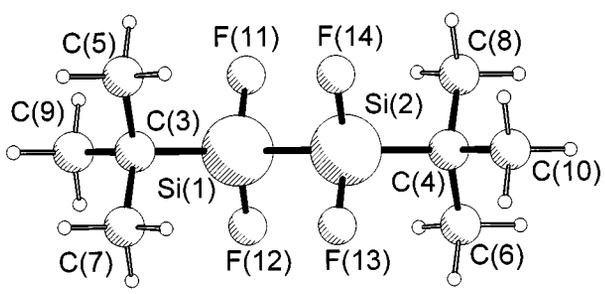

Fig. 1 Molecular structure of the *anti* conformer of $Bu^tSiF_2SiF_2Bu^t$

Table 2 Theoretical geometrical parameters for the *gauche* and *anti* conformers and transition state (T. S.) of 1,2-di-*tert*-butyltetrafluorodisilane[a]

	3-21G*/SCF			6-31G*/SCF		
	gauche	*anti*	T. S.	*gauche*	*anti*	T. S.
Si(1)–Si(2)	230.8	230.4	230.9	235.4	234.9	235.2
Si(1)–C(3)	185.3	185.1	185.3	188.0	188.0	188.0
C(3)–C(5)	155.3	155.4	155.2	154.1	154.1	155.2
C(3)–C(7)	155.3	155.4	155.3	154.1	154.1	155.3
C(3)–C(9)	155.0	155.0	155.1	154.2	154.2	155.1
C–H[b]	108.5	108.5	108.5	108.6	108.7	108.6
Si(1)–F(11)	159.2	159.6	159.4	159.6	159.9	159.6
Si(1)–F(12)	159.9	159.6	159.8	160.0	159.9	160.0
Si(2)–Si(1)–C(3)	113.8	114.1	115.3	117.3	117.6	117.4
Si(1)–C(3)–C(5)	109.2	108.7	109.9	109.7	109.6	109.7
Si(1)–C(3)–C(7)	108.9	108.7	109.0	109.5	109.6	109.5
Si(1)–C(3)–C(9)	110.6	111.1	110.0	109.0	108.9	108.9
Si(2)–Si(1)–F(11)	111.0	108.5	109.4	108.0	107.6	107.6
Si(2)–Si(1)–F(12)	106.8	108.5	107.7	107.5	107.6	107.6
C–C–H[b]	110.4	110.7	110.5	111.2	111.2	111.2
C(3)–Si(1)–Si(2)–C(4)	123.3	180.0	151.9	138.3	180.0	147.4

[a] All distances in pm, all angles in °. See Fig. 1 for atom numbering. [b] Weighted average of all values.

Table 3 Relative energies (kJ mol^{-1}) of the *anti* and *gauche* conformers of 1,2-di-*tert*-butyltetrafluorodisilane and the barrier between these conformers[a]

	Anti	*Gauche*	Barrier[b]
3-21G*/SCF	0(0)	−0.88 (0.23)	2.44 (1.27)
6-31G*/SCF	0(0)	1.20 (1.45)	0.03 (−0.22)
6-31G*/MP2[c]	0(0)	0.64 (0.89)	0.48 (0.25)

[a] Values in parentheses have been corrected for ZPE. [b] The barrier is calculated relative to the *gauche* conformer. [c] Single point calculation performed using the optimised geometry and ZPE correction obtained at the 6-31G*/SCF level.

Table 4 Experimentally observed infrared and Raman spectra (<3000 cm^{-1}) of Bu^{t}SiF$_2$SiF$_2$Bu^t

IR, liquid, *T* 25 °C	Raman, solid, *T* −190 °C	Raman, liquid, *T* 25 °C
2961vs	2958s	2957m
2941vs	2938vs	2938s
2895m	2903vs	2902vs
2810vw	2865vs	2868vs
2785vw	2786m	2790m
2757vw	2717m	2723m
2727vw	1469ms	1469m
1473vs	1447ms	1447m
1470 (sh)	1400vw	1398vw
1445vw	1369vw	1369vw
1397w	1230ms	1230ms
1369m	1190m	1190m
1260w	1008w	1010w
1225vw	942m	944m
1186w	886vw	890vw
1005m	857w	860w
965 (sh?)	846vw?	844vw?
942m	825ms	825ms
900vs		803vw?
860 (sh)	673m	671s
846vs	516ms	518vs
804vs	401w	400w
666w	369w	368w
606vs		345vw?
422vs	319w	315vw
362ms		302vw
347ms	270 (sh)	
	257w	253m
	224m	218m
	196ms	196s
		133 (sh)
	117m	
		105m
	34ms	

Key: vw = very weak, w = weak, m = medium, ms = medium strong, s = strong, vs = very strong, sh = shoulder.

was calculated to be 151.9 and 147.4° at the 3-21G*/SCF and 6-31G*/SCF levels. In the latter case, the dihedral angle in the transition state is only 9° greater than at the potential minimum.

At the 3-21G*/SCF level the two local minima on the potential energy surface are separated by only 0.23 kJ mol^{-1} when a correction for zero-point energy (ZPE) is applied (Table 3). Improving the basis set leads to an *anti* structure which is the more stable by 1.25 kJ mol^{-1} (corrected for ZPE), while an MP2 calculation undertaken using the 6-31G*/SCF optimised geometry leads to an energy separation of 0.89 kJ mol^{-1}.

The barrier to interconversion of the *anti* and *gauche* isomers was calculated using the theoretical treatments adopted for earlier calculations. At the 3-21G*/SCF level the transition state was predicted to lie only 2.44 kJ mol^{-1} above the *gauche* isomer, or 1.27 kJ mol^{-1} when corrected for ZPE (see Table 3). Improving the basis set to 6-31G* reduces the estimate of this barrier to just 0.03 kJ mol^{-1} and 0.48 kJ mol^{-1} at the SCF and MP2

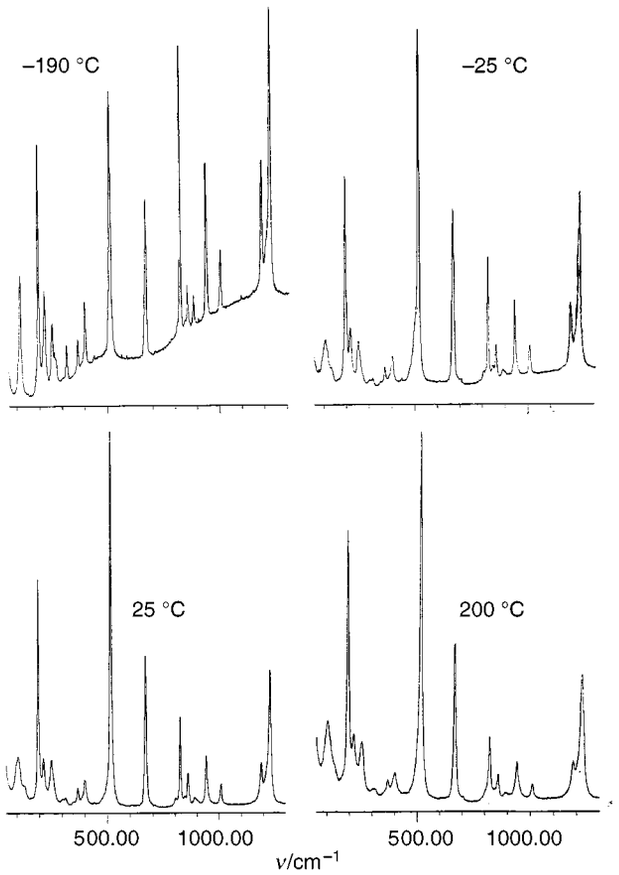

Fig. 2 Raman spectra of liquid (−25, 25 and 200 °C) and solid (−190 °C) Bu^{t}SiF$_2$SiF$_2$Bu^t

levels, respectively, when no correction for ZPE is applied. When the effects of ZPE are taken into consideration, the barrier to interconversion between these two conformers is predicted to lie slightly below the ground state vibrational level at the 6-31G*/SCF level, but just 0.25 kJ mol^{-1} above the ground vibrational state at the MP2 level. These results imply that the *gauche* conformer represents either a quasi-minimum or a very shallow well on the potential energy surface. It is, therefore unlikely to be observable, experimentally, but the torsional vibration about the Si–Si bond is likely to have a large amplitude.

Vibrational spectroscopy and normal coordinate analysis (NCA)

To investigate the rotational isomerism of 1,2-di-*tert*-butyltetrafluorodisilane further, infrared (25 °C) and Raman spectra of liquid (−25, 25, 100 and 200 °C), and solid (−190 °C) samples were recorded. Values of observed frequencies are presented in Table 4 together with scaled and unscaled *ab initio* frequencies, while selected spectra are shown in Fig. 2. The positions and relative intensities of bands in the Raman spectra of the liquid were found to be unaffected over a temperature range of −25 to 200 °C, suggesting that only one conformer is present, in agreement with the *ab initio* predictions. Furthermore, comparison of IR and Raman spectra reveals that the mutual-exclusion rule is obeyed. This strongly suggests that only the *anti* conformer contributes to the vibrational spectra, since all bands assignable to the *gauche* conformer (C_2 symmetry) should be both IR and Raman active. Moreover, theoretically predicted intensities for the *gauche* conformer indicate that some bands should be strong in both IR and Raman spectra.

A normal coordinate analysis (NCA) and potential energy distribution (PED) analysis were performed using the *ab initio* optimised geometry and unscaled harmonic *ab initio* symmetry

Table 5 Observed and calculated wavenumbers and potential energy distribution (PED) for *anti* $Bu^tSiF_2SiF_2Bu^t$*

Species	Vibration no.	Approximate description	*Ab initio* unscaled	*Ab initio* scaled by 0.92	Observed	PED
A_g(Raman)	ν_1	ρ_1CH_3	1369	1260	1230	65(1), 16(9), 12(7)
	ν_2	ρ_2CH_3	1330	1224	1190	57(2), 34(4), 10(10)
	ν_3	ρ_3CH_3	1128	1038	1010	87(3)
	ν_4	$\nu_{asym}CC_3$	1028	946	944	60(4), 30(2), 10(3)
	ν_5	$\nu_{sym}SiF_2$	928	854	860	87(5)
	ν_6	$\nu_{sym}CC_3$	890	820	825	58(6), 20(7), 18(1)
	ν_7	νSiC	719	662	671	27(7), 26(6), 22(13), 21(8)
	ν_8	νSiSi	555	511	518	27(9), 19(8), 11(13), 11(7)
	ν_9	$\delta_{sym}CC_3$	429	395	400	25(9), 19(10), 17(14), 11(11)
	ν_{10}	$\delta_{asym}CC_3$	391	360	368	62(10), 17(11)
	ν_{11}	δSiF_2	267	246	253	43(11), 22(12)
	ν_{12}	ρCC_3	232	214	218	35(12), 25(13), 16(9), 15(7)
	ν_{13}	γSiF_2	212	195	196	47(8), 26(13), 18(11)
	ν_{14}	δSiSiC	109	101	105	79(14), 26(12), 15(11)
B_g(Raman)	ν_{15}	ρ_1CH_3	1331	1225	1190	58(15), 33(18), 10(20)
	ν_{16}	ρ_2CH_3	1126	1036	1010	88(16)
	ν_{17}	ρ_3CH_3	1058	974	—	100(17)
	ν_{18}	$\nu_{asym}CC_3$	1029	947	944	60(18), 30(15), 10(16)
	ν_{19}	$\nu_{asym}SiF_2$	965	888	890	101(19)
	ν_{20}	$\delta_{asym}CC_3$	433	399	400	49(20), 14(23), 12(21)
	ν_{21}	ρCC_3	150	139	133	60(21), 33(23), 33(22)
	ν_{22}	τSiF_2	210	194	196	67(22), 23(23), 11(21)
	ν_{23}	ρSiF_2	336	310	315	44(20), 28(23), 19(21)
A_u(IR)	ν_{24}	ρ_1CH_3	1330	1224	1186	58(24), 33(27), 10(29)
	ν_{25}	ρ_2CH_3	1125	1036	1005	88(25)
	ν_{26}	ρ_3CH_3	1058	974	965?	100(26)
	ν_{27}	$\nu_{asym}CC_3$	1029	947	942	60(27), 29(24)
	ν_{28}	$\nu_{asym}SiF_2$	974	897	900	100(28)
	ν_{29}	$\delta_{asym}CC_3$	424	391	—	61(29), 11(24), 10(30)
	ν_{30}	ρCC_3	317	292	—	34(30), 34(29)
	ν_{31}	τSiF_2	149	138	—	73(31), 56(30)
	ν_{32}	ρSiF_2	108	100	—	97(32), 30(31)
B_u(IR)	ν_{33}	ρ_1CH_3	1367	1258	1225	64(33), 16(40), 12(39)
	ν_{34}	ρ_2CH_3	1327	1221	1186	58(34), 33(36), 10(41)
	ν_{35}	ρ_3CH_3	1124	1034	1005	89(35)
	ν_{36}	$\nu_{asym}CC_3$	1027	945	942	61(36), 30(34)
	ν_{37}	$\nu_{sym}SiF_2$	916	843	846	58(37), 18(38), 18(39), 11(33)
	ν_{38}	$\nu_{sym}CC_3$	866	797	804	52(38), 38(37)
	ν_{39}	νSiC	641	590	606	47(39), 24(38), 14(40)
	ν_{40}	$\delta_{sym}CC_3$	388	358	362	35(40), 34(41)
	ν_{41}	$\delta_{asym}CC_3$	457	421	422	29(44), 17(41), 14(43), 13(40)
	ν_{42}	δSiF_2	366	337	347	43(42), 38(41)
	ν_{43}	ρCC_3	269	248	—	41(42), 14(43), 14(40), 11(39)
	ν_{44}	γSiF_2	200	184	—	52(44), 63(43)
	ν_{45}	δSiSiC	64	59	—	101(45), 11(42)

* Values in parentheses refer to the contributing modes, only modes with weights above 10% are reported.

force constants (6-31G*/SCF) of the *anti* conformer by employing the FG-formalism of Wilson.[19] This allowed all low-frequency modes to be assigned satisfactorily (see Table 5). The *ab initio* symmetry force constants were obtained by transforming the Cartesian Hessian matrix into a force field defined by 90 symmetry coordinates, which are linear combinations of 172 internal coordinates. Redundancies were removed by choosing symmetry coordinates which are orthogonal to the redundancy conditions. The symmetry coordinates can be obtained from the authors upon request. Since high-frequency modes ($\nu_{sym}CH_3$, $\nu_{asym}CH_3$, $\delta_{sym}CH_3$ and $\delta_{asym}CH_3$) and torsional vibrations are only of limited interest and couple negligibly with other modes, they were omitted from the NCA. Rocking CH vibrations were incorporated as they are strongly coupled with C–C stretching modes. The vibrational problem for $Bu^tSiF_2SiF_2Bu^t$ is thus simplified to equation (1).

$$C_{2h}: \Gamma_{vibration} = 14A_g(\text{Raman}) + 9B_g(\text{Raman}) + 9A_u(\text{IR}) + 13B_u(\text{IR}) \quad (1)$$

Table 5 shows experimental, unscaled and scaled *ab initio* frequencies for the *anti* conformer, with their assignments to symmetry coordinates and potential-energy distributions (PED). From these values it can be seen that the NCA for $Bu^tSiF_2SiF_2Bu^t$ did not allow an unambiguous description of the experimental and calculated vibrational frequencies from the chosen set of symmetry coordinates. This occurs mainly because some off-diagonal symmetry force constants are overestimated at the 6-31G*/SCF level of theory. The coupling between the modes $\delta_{sym}CC_3$, $\delta_{asym}CC_3$, δSiF_2, ρCC_3 and γSiF_2 is unusually large, especially for B_u modes, and so the approximate descriptions of these modes in Table 5 are more or less arbitrary. In the A_g symmetry species the Si–Si stretching mode is highly coupled with the $\delta_{sym}CC_3$, νSiC and γSiF_2 modes. The theoretical Si–Si stretching force constant (unscaled 212, scaled 179 N m^{-1}) is smaller than one would predict from the spectroscopic force constants reported for Si_2F_6 and Si_2Me_6 (240 and 165 N m^{-1}, respectively).[20,21] Based on the assumption that a *tert*-butyl group has approximately the same influence on the Si–Si force constant as a methyl group, a value of 215 N m^{-1} can be interpolated for the Si–Si stretching force constant of $Bu^tSiF_2SiF_2Bu^t$. Indeed, a value of 220 N m^{-1} has been reported previously for $Bu^tSiF_2SiF_2Bu^t$.[6]

Electron diffraction analysis

On the basis of *ab initio* calculations detailed above, two differ-

Table 6 Refined and calculated geometric parameters for $Bu^tSiF_2SiF_2Bu^t$ (distances in pm, angles in °) from the GED study[a]

No.	Parameter	GED (r_a)	6-31G*/SCF (r_e)[b]
p_1	Si–Si	234.6(6)	234.9
p_2	Si–C	187.2(3)	188.0
p_3	Si–F	160.0(2)	159.9
p_4	C–C	153.7(3)	154.1
p_5	C–H	113.5(2)	108.7
p_6	Si–Si–F	108.7(3)	108.0
p_7	F–Si–F	107(2)	105.3
p_8	Si–Si–C	114.6(7)	117.6
p_9	C–C–C	110.2(5)	109.6
p_{10}	C–C–H	109.5(10)	111.2
p_{11}	Si–C–C–H	180 (fixed)	180.0
p_{12}	Si–Si–C–C	192.5(17)	180.0
p_{13}	C–Si–Si–C (*anti*)	184(7)	180.0
p_{14}	C–Si–Si–C (*gauche*)	152(3)	138.3
p_{15}	Tilt C_3C–Si	3.7(6)	0.6

[a] Figures in parentheses are the estimated standard deviations of the last digits. See text for parameter definitions. [b] Only values for the *anti* conformer are reported here.

Table 7 Selected interatomic distances and mean amplitudes of vibration for $Bu^tSiF_2SiF_2Bu^t$ from the GED study*

Atom pair	r_a /pm		u/pm
Si–Si	234.6(6)	u_1	6.4(6)
Si–C	187.2(3)	u_2	5.1(3)
Si–F	160.0(2)	u_3	4.2(2)
C–C	153.7(3)	u_4	3.3 (tied to u_3)
C–H	113.5(2)	u_5	9.8(2)
Si(1)···C(9)	273.9(14)	u_6	8.3(7)
Si(1)···C(5, 7)	283.3(10)	u_7	8.5 (tied to u_6)
Si(1)···C(4)	355.9(11)	u_8	10.7(14)
Si(1)···C(6)	378.3(26)	u_9	13.2(32)
Si(1)···C(8)	407.7(22)	u_{10}	13.2 (tied to u_{11})
Si(1)···C(10)	486.4(7)	u_{11}	8.8(9)
Si(1)···F(13)	323.5(4)	u_{12}	10.5(4)
F(11)···F(12)	257.2(37)	u_{13}	9.3 (tied to u_1)
C(3)···C(5, 7, 9)	249.9(9)	u_{14}	7.0(9)
C(3)···F(11)	282.7(11)	u_{15}	20.7(43)
C(5)···F(11)	344.4(12)	u_{16}	34.2(49)
C(5)···F(12)	416.8(9)	u_{17}	9.8(11)
C(7)···F(11)	319.8(28)	u_{18}	34.2 (tied to u_{16})
C(7)···F(12)	415.5(8)	u_{19}	9.8 (tied to u_{17})
C(9)···F(11)	305.2(17)	u_{20}	30.1 (tied to u_{16})
C(9)···F(12)	331.0(30)	u_{21}	30.6 (tied to u_{16})

* See Fig. 1 for atom numbering; all other distances were included in the refinement, but are not listed here.

ent models were used to define the atomic coordinates of 1,2-di-*tert*-butyltetrafluorodisilane for the electron diffraction refinements. These described the vapour as consisting of either the *anti* conformer only or both *anti* and *gauche* conformations. The large number of geometric parameters needed to define both models made it necessary to make a number of assumptions. Methyl and *tert*-butyl groups were assumed to have local C_{3v} and local C_3 symmetry, respectively. Similarly, local C_s symmetry was adopted for the $SiSiCF_2$ fragments. Since corresponding bond distance and bond angle parameters were predicted to differ by less than 0.5 pm and 0.5° respectively for the *anti* and *gauche* conformers at the highest level employed (6-31G*/SCF), such differences were fixed at zero during the refinements.

The structure of $Bu^tSiF_2SiF_2Bu^t$ was defined in terms of 15 independent geometric parameters; these comprised five bond lengths (Si–Si, Si–C, Si–F, C–C and C–H, p_1–p_5), five bond angles (Si–Si–F, F–Si–F, Si–Si–C, C–C–C and C–C–H, p_6–p_{10}), twist angles for methyl and *tert*-butyl groups [Si(1)–C(3)–C(9)–H and Si(2)–Si(1)–C(3)–C(9), p_{11} and p_{12}], and a dihedral angle, C(3)–Si(1)–Si(2)–C(4), for each of the *anti* and *gauche* conformations (p_{13} and p_{14}). The atom numbering is shown in Fig. 1. In addition, the local C_3 axes of the *tert*-butyl groups were allowed to deviate from the Si–C bond axis by the introduction of a tilt angle, p_{15}. A positive tilt leads to a single Si(1)–C(3)–C(9) angle and to two equivalent larger ones [Si(1)–C(3)–C(5) and Si(1)–C(3)–C(7)] for the *anti* conformer. A single tilt angle was assumed to apply for both conformers. The list of independent geometric parameters is given in Table 6.

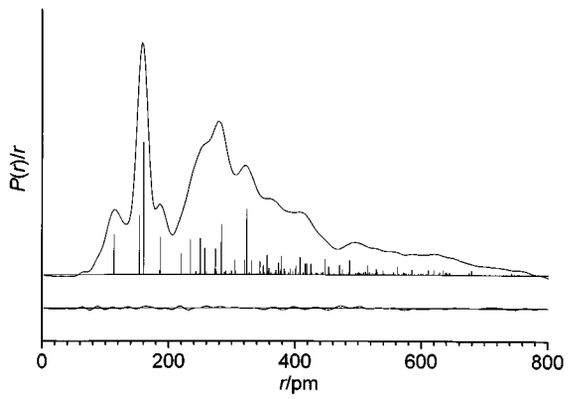

Fig. 3 Experimental and difference (experimental − theoretical) radial-distribution curves, $P(r)/r$, for $Bu^tSiF_2SiF_2Bu^t$. Before Fourier inversion the data were multiplied by $s\cdot\exp(-0.00002s^2)/(Z_F - f_F)/(Z_{Si} - f_{Si})$

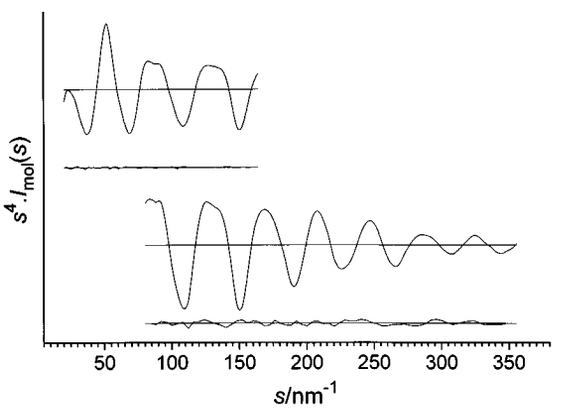

Fig. 4 Experimental and final weighted difference (experimental − theoretical) molecular-scattering intensities for $Bu^tSiFi_2SiF_2Bu^t$

The starting parameters for the r_a refinement were taken from the theoretical geometries optimised at the 6-31G*/SCF level. Theoretical (6-31G*/SCF) Cartesian force fields were obtained for both local minima and converted into force fields described by a set of symmetry coordinates using the ASYM40 program.[22] The presence of a number of low-frequency vibrational modes led to overestimated predictions of the perpendicular amplitudes of vibration (k). Since these values were considered unreliable, corrections for shrinkage effects were not included.

Simultaneous refinement of geometric and vibrational parameters associated with the heavy-atom skeleton was initially attempted using the model describing the *anti* isomer only. This single-conformer model proved unsatisfactory since this description failed to give an adequate description of the large-amplitude torsional motion about the Si–Si bond. The introduction of the second (*gauche*) conformer resulted in a substantially improved fit to the experimental data. It should be noted that the improved fit associated with the inclusion of the *gauche* conformation does not necessarily imply that this conformer is present as a distinct entity in the vapour, since additional conformations may be needed to model any large amplitude motions which occur. Initial refinements using the two-conformer model were carried out assuming a weight of 66% for the *gauche* conformation based on the assumption that the two conformers are of equal energy. All geometric parameters except for p_{13}, the C–Si–Si–C dihedral angle for the *anti* con-

Table 8 Least-squares correlation matrix (×100) for $Bu^tSiF_2SiF_2Bu^t$*

	p_3	p_7	p_8	p_9	p_{10}	p_{12}	p_{14}	p_{15}	u_1	u_4	u_9	u_{12}	u_{14}	u_{16}	k_1	k_2
p_1					74											−50
p_2					63									50		
p_4	−90									69						
p_6		−86	65	−76		−73	−53						69	−70		
p_7			−84	81		62							−79	78		
p_8				−60									64	−87		
p_9						57	56		−50				−77			
p_{10}														57		−72
u_6						81					54					
u_8													58		54	
u_9								−76			50	−62				
u_{15}								−69			83					
u_{16}							54	−69								
u_{17}						−50										
k_1												50				
													57			
						52										
																65

* Only elements with absolute values >50% are shown; k_1 and k_2 are scale factors.

former (fixed at 180.0°), were then refined before determining the relative weights of the two conformations. The weight of the *gauche* conformer was thus determined to be 66 ± 10%, according to a Hamilton test at the 95% confidence level.[23]

In the final refinement the weight of the *gauche* conformer was fixed at 66% and p_{13} was allowed to refine freely so that a more complete description of the restricted rotation about the Si–Si bond could be obtained. In total 14 geometric parameters and 13 groups of vibrational amplitudes were refined. The success of the final refinement, for which $R_G = 0.035$, can be assessed on the basis of the radial distribution curve (Fig. 3) and the molecular scattering intensity curves (Fig. 4). Final refined parameters are listed in Table 6, interatomic distances and the corresponding amplitudes of vibration in Table 7 and the least-squares correlation matrix is in Table 8. Fig. 1 shows the *anti* conformer of $Bu^tSiF_2SiF_2Bu^t$ in the optimum refinement of the GED data.

Discussion

Theoretical and experimental studies show that 1,2-di-*tert*-butyltetrafluorodisilane exists as a single, *anti* conformer in the gas-phase. Although *ab initio* calculations led to the location of two non-equivalent local minima (*anti* and *gauche*), the *gauche* structure was predicted to lie within 0.3 kJ mol^{-1} of the barrier connecting the two conformers in its ground vibrational state at the 6-31G*/MP2 level, implying that this conformer should not be observable as a distinct structural entity. The theoretical investigation is supported by spectroscopic measurements which are consistent with the presence of a single conformer only. Comparison of the IR and Raman spectra reveals that the mutual-exclusion rule is obeyed, indicating that the *anti* conformer only is observed. The electron diffraction data could not be fitted on the basis of an *anti* structure alone, and the inclusion of a second conformer (*gauche*) is required to model the large torsional motion about the silicon–silicon bond. The C–Si–Si–C dihedral angles for the *anti* and *gauche* conformers refined to 184(7) and 152(3)°, values which are consistent with a large-amplitude motion over a torsional range of around 140–220° rather than a second stable conformation.

The final refined structure is in excellent agreement with that calculated at the 6-31G*/SCF level; computed bond lengths and angles generally fell within 1 pm or 1–2° of the GED values (Table 6). Observed geometric parameters are consistent with those for a number of other closely related compounds. For example, the Si–Si bond distance in 1,2-di-*tert*-butyltetrafluorodisilane [234.6(6) pm] is indistinguishable from that found for 1,2-di-*tert*-butyldisilane[24] and 1,1,2,2-tetrabromodisilane[25] [234.8(3) and 234.9(19) pm, respectively]. Although longer Si–Si bonds have previously been reported for 1,2-diiododisilane[26] and 1,1,2,2-tetraiododisilane[26] [238.0(34) and 238.9(37) pm], differences are of the order of one standard deviation. Refined values of the C–C [153.7(3) pm], Si–F [160.0(2) pm] and Si–C [187.2(3) pm] bond lengths are in excellent agreement with calculated values and compare well with other previously reported single bond lengths.[27] The measured Si–Si–C angle for 1,2-di-*tert*-butyltetrafluorodisilane [114.6(7)°] is also in good agreement with that found for 1,2-di-*tert*-butyldisilane [113.7(4)°].[24] The slight widening observed for the fluoro compound can be readily attributed to the larger electron withdrawing effect expected for fluorine as compared to hydrogen.

Acknowledgements

We thank the EPSRC for financial support of the Edinburgh Electron Diffraction Service (grant GR/K44411), for the provision of microdensitometer facilities at the Daresbury Laboratory and for the Edinburgh *ab initio* facilities (grant GR/K04194).

References

1 R. D. Miller and J. Michl, *Chem. Rev.*, 1989, **89**, 1359.
2 B. Albinsson, H. Teramae, J. W. Downing and J. Michl, *Chem. Eur. J.*, 1996, **2**, 529.
3 C. A. Ernst, L. A. Allred and M. A. Ratner, *J. Organomet. Chem.*, 1979, **178**, 119.
4 D. W. H. Rankin, in *Structures and Conformations of Non-rigid Molecules*, eds. J. Laane, B. van der Veken and H. Oberhammer, Kluwer Academic Publishers, Dordrecht, 1993.
5 B. Albinsson and J. Michl, *J. Phys. Chem.*, 1996, **100**, 3418.
6 B. Reiter and K. Hassler, *J. Organomet. Chem.*, 1994, **21**, 467.
7 M. J. Frisch, G. W. Trucks, H. B. Schlegel, P. M. W. Gill, B. G. Johnson, M. A. Robb, J. R. Cheesman, T. A. Keith, G. A. Petersson, J. A. Montgomery, K. Raghavachari, M. A. Al-Laham, V. G. Zakrzewski, J. V. Ortiz, J. B. Foresman, J. Cioslowski, B. B. Stefanov, A. Nanayakkara, M. Challacombe, C. Y. Peng, P. Y. Ayala, W. Chen, M. W. Wong, J. L. Andres, E. S. Replogle, R. Gomperts, R. L. Martin, D. J. Fox, J. S. Binkley, D. J. Defrees, J. Baker, J. P. Stewart, M. Head-Gordon, C. Gonzalez and J. A. Pople, GAUSSIAN 94, Revision C.2, Gaussian Inc., Pittsburgh, PA, 1995.
8 J. S. Binkley, J. A. Pople and W. J. Hehre, *J. Am. Chem. Soc.*, 1980, **102**, 939.

9 M. S. Gordon, J. S. Binkley, J. A. Pople, W. J. Pietro and W. J. Hehre, *J. Am. Chem. Soc.*, 1982, **104**, 2797.
10 W. J. Pietro, M. M. Francl, W. J. Hehre, D. J. Defrees, J. A. Pople and J. S. Binkley, *J. Am. Chem. Soc.*, 1982, **104**, 5039.
11 W. J. Hehre, R. Ditchfield and J. A. Pople, *J. Chem. Phys.*, 1972, **56**, 2257.
12 P. C. Hariharan and J. A. Pople, *Theor. Chim. Acta*, 1973, **28**, 213.
13 M. S. Gordon, *Chem. Phys. Lett.*, 1980, **76**, 163.
14 C. M. Huntley, G. S. Laurenson and D. W. H. Rankin, *J. Chem. Soc., Dalton Trans.*, 1980, 954.
15 S. Cradock, J. Koprowski and D. W. H. Rankin, *J. Mol. Struct.*, 1981, **77**, 113.
16 A. S. F. Boyd, G. S. Laurenson and D. W. H. Rankin, *J. Mol. Struct.*, 1981, **71**, 217.
17 A. W. Ross, M. Fink and R. Hildebrandt, in *International Tables for Crystallography*, ed. A. J. C. Wilson, Kluwer Academic Publishers, Dordrecht, 1992, vol. C, p. 245.
18 W. J. Hehre, L. Radom, P. V. R. Schleyer and J. A. Pople, *Ab Initio Molecular Orbital Theory*, Wiley, New York, 1986.
19 E. B. Wilson, J. C. Decius and P. C. Cross, *Molecular Vibrations*, McGraw-Hill, New York, 1955.
20 F. Höfler, S. Waldhör and E. Hengge, *Spectrochim. Acta, Part A*, 1972, **28**, 29.
21 F. Höfler, *Monatsh. Chem.*, 1976, **107**, 893.
22 L. Hedberg and I. M. Mills, *J. Mol. Spectrosc.*, 1993, **160**, 117.
23 W. C. Hamilton, *Acta Crystallogr.*, 1965, **18**, 502.
24 D. Hnyk, R. S. Fender, H. E. Robertson, D. W. H. Rankin, M. Bühl, K. Hassler and K. Schenzel, *J. Mol. Struct.*, 1995, **346**, 215.
25 H. Thomassen, K. Hagen, R. Stølevik and K. Hassler, *J. Mol. Struct.*, 1986, **147**, 331.
26 E. Røhmen, K. Hagen, R. Stølevik, K. Hassler and M. Pöschl, *J. Mol. Struct.*, 1991, **244**, 41.
27 See, for example, N. W. Mitzel, B. A. Smart, A. J. Blake, H. E. Robertson and D. W. H. Rankin, *J. Phys. Chem.*, 1996, **100**, 9339.

Received 1*st April* 1997; *Paper* 7/02185B